ELSEVIER

Biophysical Chemistry 125 (2007) 184–190

Biophysical Chemistry

http://www.elsevier.com/locate/biophyschem

Amyloid fibrils formation and amorphous aggregation in concanavalin A

Valeria Vetri [a,c], Claudio Canale [b], Annalisa Relini [b], Fabio Librizzi [a,*], Valeria Militello [a,c], Alessandra Gliozzi [b], Maurizio Leone [a,c]

[a] *Università di Palermo, Dipartimento di Scienze Fisiche ed Astronomiche, Via Archirafi 36, 90123 Palermo, Italy*
[b] *Università di Genova, Dipartimento di Fisica, Via Dodecaneso 33, 16146 Genova, Italy*
[c] *Consiglio Nazionale delle Ricerche, Istituto di Biofisica, Sez. di Palermo, Via U. La Malfa 153, 90146 Palermo, Italy*

Received 7 July 2006; accepted 25 July 2006
Available online 2 August 2006

Abstract

We here report an experimental study on the thermal aggregation process of concanavalin A, a protein belonging to the legume lectins family. The aggregation process and the involved conformational changes of the protein molecules were followed by means of fluorescence techniques, light scattering, circular dichroism, zeta potential measurements and atomic force microscopy. Our results show that the aggregation process of concanavalin A may evolve through two distinct pathways leading, respectively, to the formation of amyloids or amorphous aggregates. The relative extent of the two pathways is determined by pH, as amyloid aggregation is favored at high pH values (~9), while the formation of amorphous aggregates is favored at low pH (~5). At difference from amorphous aggregation, the formation of amyloid fibrils requires significant conformational changes on the protein, both at secondary and tertiary structural level. To our knowledge, this is the first observation of amyloid fibrils from concanavalin A.

Keywords: Concanavalin A; Protein aggregation; Amyloids; Thioflavin T fluorescence; Atomic force microscopy; Circular dichroism

1. Introduction

When exposed to destabilizing conditions, proteins may undergo unfolding and/or aggregation processes. Beyond their intrinsic scientific relevance, at present these phenomena are extensively studied, since they result to be involved in many areas of biomedical and biotechnological research. It is well known that several human pathologies, in particular neurodegenerative disorders such as Alzheimer's and Parkinson's diseases, are characterized by the formation and deposition of large amounts of insoluble material, resulting from the aggregation of misfolded proteins and peptides [1–6]. These aggregates are mainly composed of fibrillar structures, known as amyloid fibrils. In spite of the absence of any similarity in the sequence and in the conformation of the proteins involved, all amyloid fibrils share common morphological features. In general they are formed by protofilaments in which the protein molecules are arranged in β-strands perpendicular to the elongation axis. The protofilaments may associate or twist around each other, thus forming fibrils of larger diameter [7,8]. Until a few years ago, it was assumed that pathogenic effects in amyloid diseases were mainly due to mature amyloid fibrils. Instead, although the massive accumulation of amyloid deposits may obviously be a source of clinical symptoms, increasing evidences showed that prefibrillar aggregates rather than mature fibrils are mainly responsible of cytotoxic effects [9].

Under appropriate destabilizing conditions, even proteins and peptides not related to any kind of disease can be involved in the formation of amyloid fibrils, thus suggesting that the tendency to form amyloid aggregates could be a generic property of any polypeptide chain [10]. Therefore, amyloid aggregation would appear as an alternative pathway, in kinetic competition with the normal protein folding [11].

Conformational changes are commonly recognized to play a pivotal role in the aggregation processes, since they lead to the exposure of normally buried regions, such as hydrophobic groups, which may promote the onset of new intermolecular interactions [6,12–15]. Depending on the details of the external conditions (temperature, pH, solution composition...) different

* Corresponding author.
E-mail address: librizzi@fisica.unipa.it (F. Librizzi).

0301-4622/$ - see front matter © 2006 Elsevier B.V. All rights reserved.
doi:10.1016/j.bpc.2006.07.012

conformational changes may lead to different aggregation pathways, thus resulting in structurally different supramolecular aggregates, such as amorphous aggregates or amyloid fibrils [16–18]. In particular, the nature of the aggregation process can be sizably affected by pH, since the latter can determine the initial structure and the net charge of the protein and, therefore, the extent to which different kinds of interactions are involved. In this scenario, the investigation of the pH dependence of the aggregation process of a suitable protein can help to clarify the mechanisms leading to different kinds of aggregation.

Concanavalin A (ConA) is an "all-β" protein belonging to the legume lectins family. Its quaternary structure is governed by a dimer–tetramer equilibrium, depending on pH and temperature. In particular, the protein is essentially a tetramer at physiological pH and a dimer at pH values less than 6 [19,20]. The tetramer is constituted by two identical dimers, perpendicularly joined through the central part of their back-sheets. Each monomer presents a saccharide binding site and two metal sites, binding respectively Ca^{2+} and Mn^{2+} [21–24]; the monomer is constituted by 12 β-sheets, and its tertiary structure is described as a "jelly roll" motif [25]. Altogether, as reported by Emsley et al. [26], the structure of ConA is remarkably similar to the structure of pentameric human serum amyloid P component, a protein which binds to all forms of amyloid fibrils and is universally found in amyloid deposits. At pH between 8 and 9, ConA undergoes an apparent irreversible conformational transition, resulting in protein aggregation and precipitation [27,28].

The study of the aggregation process of this "all β" protein is interesting also in view of the observation that the amyloid core structure mainly consists of β-sheets and that many short peptides with high "β-sheet propensity" display a strong tendency to form amyloid fibrils [29,30]. Furthermore, ConA is a widely used tool in several research fields, spanning from the study of protein–carbohydrate interactions (see e.g. [31–34]) to biomedical applications, where the protein is extensively used in model systems for its ability to induce liver injury (see e.g. [35–39]). Therefore, a characterization of its aggregation pathways may be useful for many scientific applications.

It is worth to note that ConA has been reported to be able to induce programmed cell death on cortical neurons, by a mechanism which involves the cross-linking of specific membrane receptors, and displays remarkable analogies with programmed cell death induced by the amyloid-β peptide (Aβ), universally known for its role in Alzheimer's disease [40,41].

We report here a kinetic study of the thermal aggregation of ConA in the low concentration regime, at different pH values. The formation of amyloid aggregates was monitored by means of Thioflavin T (Th T) fluorescence. As it is well known, in the presence of amyloid aggregates Th T shows a bright fluorescence band, whose intensity appears to be, in a good approximation, linearly dependent on the amount of aggregates present in the sample [42,43]. A moderate irreversible increase in Th T fluorescence has been observed during the thermal aggregation of ConA at pH 6 [44]. Complementary information on the extent of aggregation was obtained by the elastic scattering of the fluorescence excitation light. 8-Anilino-1-naphthalene-sulfonate (ANS) was used as a probe of changes involving hydrophobic regions already present in the protein structure or eventually formed during the evolution of the aggregation process. Changes at the secondary structure level were followed by means of far-UV circular dichroism (CD). Zeta potential measurements yielded information about changes in protein surface charge. Finally, aggregate morphology was investigated by atomic force microscopy (AFM).

2. Materials and methods

2.1. Sample preparation

ConA (type IV, L7647) ANS and Th T were purchased from Sigma Aldrich and used without further purification. All the measurements were performed in phosphate buffer 0.1 M, at pH 5.1, 6.2, 7.2, 8.3 and 8.9. Protein concentration was determined spectrophotometrically and was 0.5 mg/ml. Each solution was freshly prepared and filtered just before the measurements through 0.22 μm filters. ConA aggregation was studied at 40 °C. ANS and Th T were dissolved in the samples at a concentration of 24 μg/ml and 13.3 μg/ml, respectively.

2.2. Spectral measurements

Fluorescence spectra were measured using a Jasco FP-6500 instrument equipped with a Jasco ETC-273T peltier as temperature controller. Samples were positioned in a 1 cm path cuvette and, after 3 min for thermal equilibration, emission spectra were recorded. All fluorescence spectra were performed with emission and excitation bandwidth of 3 nm, scan-speed of 100 nm/min, integration time of 1 s, and recorded at 0.5 nm intervals. Light scattering at 90° was also measured as the maximum of the elastic peaks of excitation light.

ANS and Th T emission spectra were detected using an excitation wavelength of 380 nm and 440 nm, respectively.

Absorption measurements were made using a Jasco V-570 Spectrophotometer.

Circular dichroism (CD) measurements were made using a Jasco J-715 spectropolarimeter, in the far-UV range, using a 0.5 mm path quartz couvette. Temperature was controlled by a Jasco PCT 348WI peltier. CD spectra were recorded with a scan speed of 50 nm/min and a bandwidth was 1 nm. To follow the kinetics, no averaging of scans was employed.

2.3. AFM measurements

AFM images were acquired in tapping mode using a Dimension 3000 microscope (Digital Instruments–Veeco, Santa Barbara, CA), equipped with a 'G' scanning head (maximum scan size 100 μm) and driven by a Nanoscope IIIa controller. For imaging in air, single beam uncoated silicon cantilevers (type OMCL-AC, Olympus, and RTESP, Veeco) were used. The drive frequency was around 300 kHz and the scan rate was between 0.3 and 0.8 Hz. The 0.5 mg/ml ConA solution (prepared as described above) was diluted 400 times and a small aliquot (20 μl) was deposited on freshly cleaved mica. The sample was dried under mild vacuum and imaged in air.

2.4. Zeta potential measurements

Zeta potential was measured at 25 °C with a Zetasizer Nano ZS (Malvern Instruments) at a protein concentration of 0.5 mg/ml in phosphate buffer. Each measurement was performed on a freshly extracted aliquot of the protein sample kept at 40 °C for aggregation. The data reported are the mean of at least five different measurements. Error bars represent the 95% confidence interval according to Student's statistics.

2.5. Dynamic light scattering measurements

Protein size in solution in the native state was measured by dynamic light scattering employing a Zetasizer Nano ZS (Malvern Instruments). To avoid protein aggregation, measurements were performed at 15 °C. Protein concentration was 0.5 mg/ml in phosphate buffer.

3. Results

Fig. 1a shows the Th T fluorescence of ConA as a function of time during the aggregation process, at different pH values and at a temperature of 40 °C. Fig. 1b shows the evolution of the scattered light intensity for the same samples. Data reported in Fig. 1b clearly indicate the formation of large aggregates at all the pH values investigated. At difference, Th T fluorescence intensity (Fig. 1a) shows a signal increase only for the samples at the highest pH values. Taken together, these data suggest the existence of two distinct aggregation pathways, leading respectively to amorphous or amyloid-like aggregates. The relative extent of the two aggregation pathways is determined by the pH, with a predominance of amorphous aggregation at low pH, close to the isoelectric point of the protein, and amyloid-like aggregation at high pH. Data corresponding to the highest pH values show that the scattered light intensity (Fig. 1b) is still growing even after when Th T fluorescence (Fig. 1a) has reached the final plateau (see for instance the data relative to the sample at pH 8.9). This can be explained either by a further association of already formed amyloid-like aggregates or by the occurrence of the amorphous aggregation pathway also at high pH.

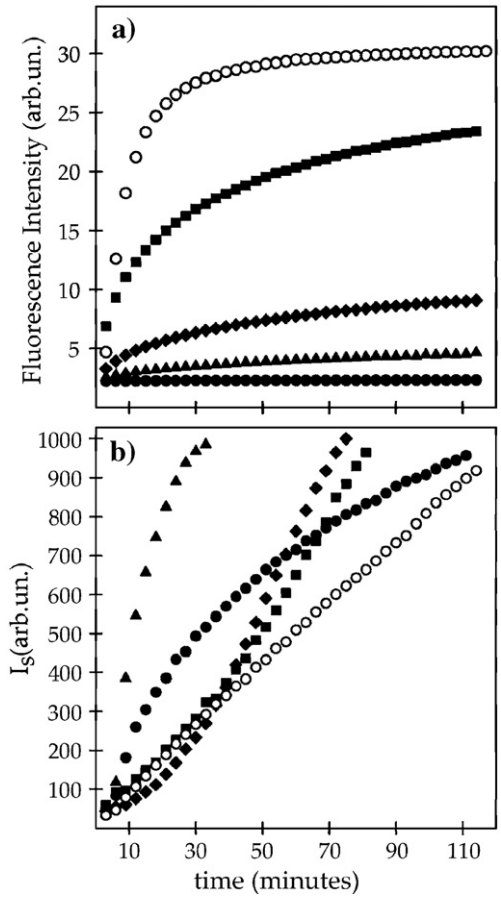

Fig. 1. Th T fluorescence (a) and elastic scattering intensity at $\lambda = 440$ nm (b), as a function of time for the samples at pH 5.1 (●), 6.2 (▲), 7.0 (◆), 8.2 (■), and 8.9 (○). Elastic scattering is measured on the excitation light of Th T fluorescence, thus, for each pH value, the data in the two panels are obtained in a single experiment.

To obtain information about the native conformation of ConA at pH 5.1 and 8.9, we measured the protein size by dynamic light scattering in solution and by atomic force microscopy after sample deposition on a mica substrate. Light scattering measurements were performed at 15 °C to avoid aggregation and yielded a size of 84 ± 14 nm at pH 5.1, while at pH 8.9 a value of 10 ± 2 nm was found. The value obtained at pH 5.1 is much larger than the expected protein size; this indicates that aggregates are already present at this pH; on the contrary, within the experimental errors, the value obtained at pH 8.9 is compatible with the absence of aggregation. In fact, the maximum dimer extension is slightly less than 8 nm, as it can be deduced from crystallographic structures (for the dimer form, 1APN from the Protein Data Bank) [45]; the tetramer size is still determined by the dimer size, as the tetrameric form (1AZD from the Protein Data Bank) [46] results from the perpendicular joining of two dimers. In addition, hydration effects can slightly increase the measured protein size. The value obtained at pH 8.9 suggests that the presence of a conformational transition at this pH [28] does not seem to alter significantly the typical ConA size. The same measurements were repeated filtering the protein solution with 20 nm pore size filters instead of 0.22 μm; we obtained 9 ± 1 nm at pH 5.1 and 8 ± 1 nm at pH 8.9. Therefore, this filtration procedure is effective in removing the aggregates at pH 5.1, as the measured size turns out to be compatible with that measured at pH 8.9 in both experiments. The presence of aggregates at pH 5.1, however, does not affect the behavior of the aggregation process. In fact, filtering the protein solution with 20 nm or 0.22 μm filters results, within experimental errors, in analogous kinetic profiles, both at low and high pH (not shown). Fig. 2 shows the histograms of protein height measured from cross-sections of the AFM images obtained from the sample used in the first set of light scattering measurements. The size distributions corresponding to pH 5.1 are clearly shifted towards larger values; in particular, mean heights of 2.44 nm and 1.65 nm (with a standard error of 0.05 nm) are obtained at pH 5.1 and 8.9, respectively. As the sample was dried to facilitate its adhesion to the mica substrate, the measured heights turn out to be smaller

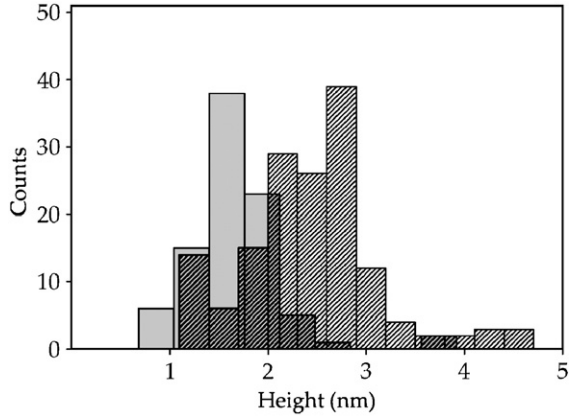

Fig. 2. ConA height distributions measured from the cross-sections of tapping mode AFM images obtained after deposition of the freshly prepared protein solution on mica. Measurements at pH 5.1 (dash) and 8.9 (gray) are compared.

than those corresponding to fully hydrated conditions. With a correction factor of ~2.5, analogous to that evaluated previously for a globular protein [47], the real mean heights would be about 6 and 4 nm respectively. In literature ConA is reported to be dimeric at pH < 6 [19,20,28]. Therefore, the broad distribution observed for our sample at pH 5.1 reflects the presence of non-native aggregates.

The morphology of the aggregates obtained incubating ConA at 40 °C and pH 8.9 or 5.1 was investigated by AFM. Fig. 3a shows the occurrence of fibrillar aggregates at pH 8.9, thus confirming that the increase in Th T fluorescence observed at this pH (see Fig. 1a) is due to the formation of amyloid fibrils. Fibril height, obtained from the height in cross section measured from AFM images, is 2.4 ± 0.2 nm. This value is comparable to those measured for amyloid fibrils of other proteins imaged in air by AFM [48]. On the contrary, at pH 5.1 (Fig. 3b) we only observed amorphous aggregates and sometimes very short rod-like structures (Fig. 3b, inset).

Fig. 4 shows the time evolution of ANS fluorescence intensity during the aggregation process, at the different pH values investigated. ANS emission is related to the presence of hydrophobic regions, and in particular a growth of the signal is an indication of the fact that new hydrophobic regions are formed during the aggregation process. We observed a more pronounced increase in the ANS fluorescence intensity for the samples at the highest pH values, with a trend similar to the one observed for Th T fluorescence data (Fig. 1a). The behavior of ANS emission indicates that the aggregation process, in particular the formation of amyloid aggregates at high pH, brings about the formation of new hydrophobic regions, probably arising from conformational changes of the protein molecules leading to a partial loss of tertiary structure.

To further investigate the conformational changes of the protein during the aggregation process, we performed far-UV circular dichroism measurements and Zeta potential measurements. Fig. 5a shows the CD spectra of the sample at pH 8.9 at different times during aggregation: a large signal decrease is observed in the range 198–230 nm, clearly indicating significant conformational changes at the secondary structure level.

Fig. 5b shows the CD signal observed at 210 nm as a function of time for the samples at the different pH values. As for the ANS emission kinetics (Fig. 4), the CD signal shows larger variations for the samples at the highest pH values, i.e. in conditions promoting the formation of amyloid fibrils. Therefore, data relative both to tertiary (ANS, Fig. 4) and to secondary (CD, Fig. 5b) structure show that the formation of amyloid fibrils at high pH requires larger conformational changes than the amorphous aggregation at low pH. This confirms the idea that amyloid aggregation is triggered by a transition to a partially folded, molten globule-like, state of proteins [6]. Remarkably, the CD signal (Fig. 5b) follows the same trend as Th T fluorescence (Fig. 1a). The two signals do not behave as an exponential rise to maximum, and can be very well fitted in terms of stretched exponentials (not shown), as recently reported for the thermal aggregation of apo–ConA [49].

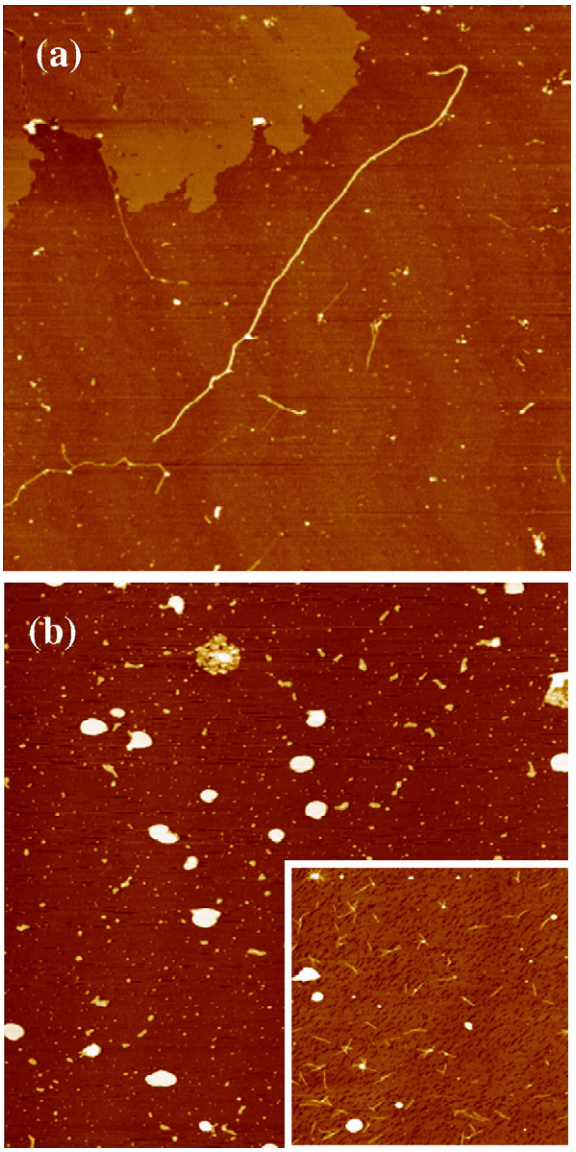

Fig. 3. Tapping mode AFM images (height data) of ConA aggregated for 40 min at 40 °C and pH 8.9 (a) or 5.1 (b). Scan size: 3.0 μm (a); 3.0 μm (b); 1.9 μm (b, inset). *Z* range = 15 nm.

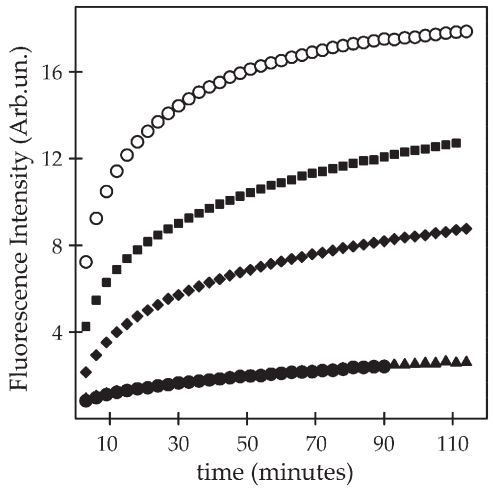

Fig. 4. ANS fluorescence emission as a function of time, for the samples at pH5.1 (●), 6.2 (▲), 7.0 (♦), 8.2 (■), and 8.9 (○). Data relative to samples at pH5.1 and 6.2 are superimposed.

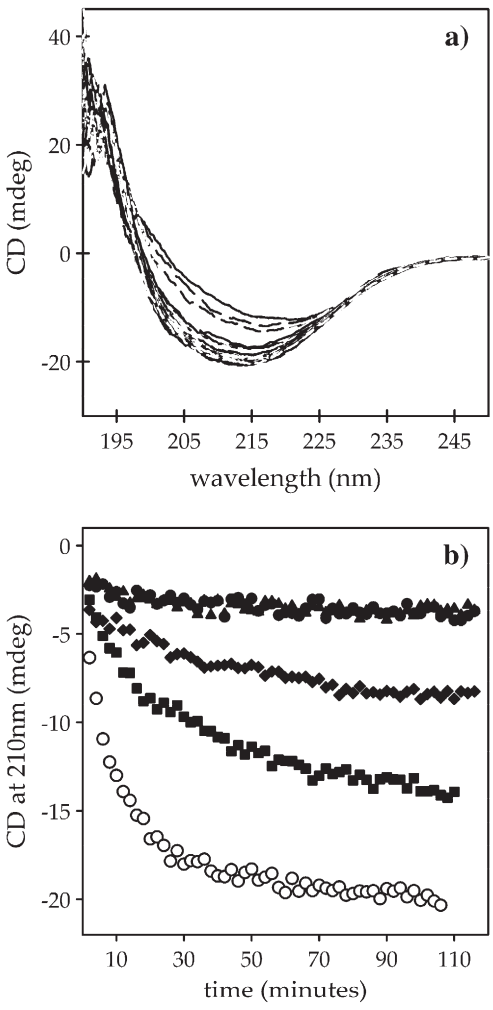

Fig. 5. Far-UV CD measurements. (a) CD spectra for the sample at pH 8.9 at different times during the aggregation process. (b) Time evolution of the CD signal at 210nm, for the samples at pH5.1 (●), 6.2 (▲), 7.0 (♦), 8.2 (■), and 8.9 (○). In panel (b), data relative to the samples at pH5.1 and 6.2 are superimposed.

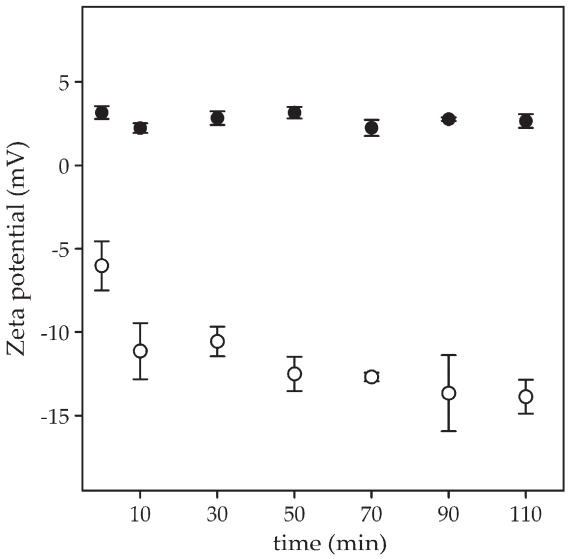

Fig. 6. Zeta potential of ConA as a function of the aggregation time at 40°C. Measurements at pH5.1 (●) and 8.9 (○) are compared.

Fig. 6 shows the Zeta potential of Con A as a function of the aggregation time. A significant decrease in the Zeta potential is observed at pH8.9, from -6 ± 1 mV to -14 ± 1 mV, indicating that the total surface charge at the sliding plane becomes, as a mean value, more negative as aggregation proceeds. On the contrary, at pH5.1 the Zeta potential is nearly constant at 2.7 mV, indicating that no change in protein surface charge occurs during amorphous aggregation. These findings are in agreement with the behavior observed with ANS fluorescence and CD and represent a further evidence of the occurrence of conformational changes in the aggregation process at high pH.

4. Discussion

We showed that at a temperature of 40°C the aggregation process of ConA can evolve through two distinct pathways, leading to the formation of amorphous aggregates or amyloid fibrils, respectively. The relative extent of the two pathways is determined by pH: amyloid fibrils formation is favored at high pH values, while amorphous aggregates arise preferentially at low pH values, close to the isoelectric point of the protein. With respect to the amorphous aggregation, the formation of amyloid fibrils requires larger conformational changes of the protein, both at the secondary and tertiary structural level, as shown in Figs. 4–6. This indicates that, at difference from amorphous aggregation, amyloid formation is triggered by the transition to a partially unfolded structure.

As far as we know, this is the first observation of amyloid aggregation in ConA. As shown, fibrillation occurs in slightly destabilizing conditions. Knowing that ConA is able to form amyloid fibrils may be important for all the medical applications of this protein [35–39], especially if we consider that fibrillation occurs in very slightly destabilizing conditions, and without using chemical destabilizers. Actually, we also observed amyloid formation at physiological conditions (37°C and

neutral pH, data not shown), although in longer times and minor extent.

As reported in the Introduction, ConA is able to induce programmed cell death in cortical neurons. According to Cribbs et al. [40], the mechanism is as follows: ConA binds to specific membrane receptors, and promotes the cross-linking of such receptors by clustering on the neuron surface. The cross-linking of the receptors, in turn, is the signal which activates a cascade of cellular processes whose termination is programmed cell death, a sort of suicide of the neuron. For this mechanism to be effective, the tendency of the involved protein to form amyloid aggregate could be important, since the clustering of the protein molecules on the neuron surface appears as a crucial step. In this respect, it is worth to note that programmed cell death can be induced also by the Aβ peptide [41], which obviously forms amyloid fibrils. For the two proteins, the process displays remarkable analogies, both in terms of neuronal induced morphological changes and in terms of generation of specific cellular products. This observation led Cribbs et al. [40] to hypothesize a common mechanism, which, if confirmed, is very like to imply the aggregation of the involved proteins. New, specifically designed experiments would be necessary to determine whether amyloid aggregation is relevant or not for the pathways leading to neuronal programmed cell death.

For multimeric amyloidogenic proteins, monomerization is often reported to be a necessary step, prior to amyloid formation. Particularly relevant is the case of transthyretin, which forms amyloid fibrils in vivo and is involved in human amyloid diseases such as senile systemic amyloidosis and familial amyloid polyneuropathy [50]. Like ConA, transthyretin is a tetramer whose subunits have a high β-sheet content. For this protein, it has been shown that the rate limiting step for amyloid formation is the dissociation to its constituent monomers [50–54]. In this respect, it is worth to note that for ConA the inter-subunits interactions which stabilize the tetrameric structure are reported to be less strong than for other lectin tetramers [24]. Therefore, tetramer dissociation could be possible, and could be involved in the pathway leading to ConA amyloid fibrillation. On the other hand, no rate limiting step is immediately evident in the fibrillation kinetics that we observed. Preliminary experiments at different concentrations and temperature (not shown) did not give definitive information at this regard, and work is in progress with other experimental techniques in order to ascertain whether monomerization is a necessary step in ConA amyloid formation. The rapidity of the process however implies that, at the difference from what was observed in transthyretin, an eventual monomeric species would be extremely unstable, and thus difficult to detect.

In our conditions the formation of amyloid fibrils proceeds without any detectable lag phase (see Fig. 1a), even at much lower protein concentration (down to 0.05 mg/ml, not shown). This suggests that the fibrillation process is not affected by any kind of cooperative mechanisms, such as heterogeneous nucleation, which have been shown to be important for other amyloidogenic proteins [55–58]. A possible scenario is that ConA fibrillation process proceeds by a simple non-cooperative elongation mechanism, as observed for the fibrillation of the Aβ peptide at low pH [59].

Acknowledgements

This work was partly supported by a national project (PRIN2005) of the Italian Ministry of University Research.

References

[1] J.D. Harper, P.T. Lansbury, Models of amyloid seeding in Alzheimer's disease and scrapie: mechanistic truths and physiological consequences of the time-dependent solubility of amyloid proteins, Annu. Rev. Biochem. 66 (1997) 385–407.
[2] J.W. Kelly, The alternative conformations of amyloidogenic proteins and their multi-step assembly pathways, Curr. Opin. Struct. Biol. 8 (1998) 101–106.
[3] V. Bellotti, P. Mangione, G. Merlini, Immunoglobulin light chain amyloidoses. The archetype of structural and pathogenic variability, J. Struct. Biol. 130 (2000) 280–289.
[4] C. Rochet, P.T. Lansbury, Amyloid fibrillogenesis: themes and variations, Curr. Opin. Struct. Biol. 10 (2000) 60–68.
[5] J. Collinge, Prion diseases of humans and animals: their causes and molecular basis, Annu. Rev. Neurosci. 24 (2001) 519–550.
[6] V.N. Uversky, A.L. Fink, Conformational constraints for amyloid fibrillation: the importance of being unfolded, Biochim. Biophys. Acta 1698 (2004) 131–153.
[7] J.L. Jiménez, J.I. Guijarro, E. Orlova, J. Zurdo, C.M. Dobson, M. Sunde, H.R. Saibil, Cryo-electron microscopy structure of an SH3 amyloid fibril and model of the molecular packing, EMBO J. 18 (1999) 815–821.
[8] L.C. Serpell, J. Berriman, R. Jakes, M. Goedert, R.A. Crowther, Fiber diffraction of synthetic α-synuclein filaments shows amyloid-like cross-β conformation, Proc. Natl. Acad. Sci. U. S. A. 97 (2000) 4897–4902.
[9] M. Stefani, Protein misfolding and aggregation: new examples in medicine and biology of the dark side of the protein world, Biochim. Biophys. Acta 1739 (2004) 5–25.
[10] M. Fandrich, C.M. Dobson, The behaviour of polyamino acids reveals an inverse side chain effect in amyloid structure formation, EMBO J. 21 (2002) 5682–5690.
[11] F. Chiti, N. Taddei, F. Baroni, C. Capanni, M. Stefani, G. Ramponi, C.M. Dobson, Kinetic partitioning of protein folding and aggregation, Nat. Struct. Biol. 9 (2002) 137–143.
[12] R. Khurana, J.R. Gillespie, A. Talapatra, L.J. Minert, C. Ionescu-Zanetti, I. Millett, A.L. Fink, Partially folded intermediates as critical precursors of light chain amyloid fibrils and amorphous aggregates, Biochemistry 40 (2001) 3525–3535.
[13] V. Militello, V. Vetri, M. Leone, Conformational changes involved in thermal aggregation processes of bovine serum albumin, Biophys. Chemist. 105 (2003) 133–141.
[14] S.M. Vaiana, A. Emanuele, M.B. Palma-Vittorelli, M.U. Palma, Irreversible formation of intermediate BSA oligomers requires and induces conformational changes, Proteins 55 (2004) 1053–1062.
[15] V. Vetri, V. Militello, Thermal induced conformational changes involved in the aggregation pathways of beta-lactoglobulin, Biophys. Chem. 113 (2005) 83–91.
[16] D.R. Booth, M. Sunde, V. Bellotti, C.V. Robinson, W.L. Hutchinson, P. E. Fraser, P.N. Hawkins, C.M. Dobson, S.E. Radford, C.C.F. Blake, M. B. Pepys, Instability, unfolding and aggregation of human lysozyme variants underlying amyloid fibrillogenesis, Nature 385 (1997) 787–793.
[17] S. Arai, M. Hirai, Reversibility and hierarchy of thermal transition of hen egg-white lysozyme studied by small-angle X-ray scattering, Biophys. J. 76 (1999) 2192–2197.
[18] D. Hamada, C.M. Dobson, A kinetic study of beta-lactoglobulin amyloid fibril formation promoted by urea, Protein Sci. 11 (2002) 2417–2426.

[19] D.F. Senear, D.C. Teller, Effects of saccharide and salt binding on dimer–tetramer equilibrium of concanavalin A, Biochemistry 20 (1981) 3076–3083.
[20] L. Bhattacharyya, S.H. Koenig, R.D. Brown, C.F. Brewer, Interactions of asparagine-linked carbohydrates with concanavalin A. Nuclear magnetic relaxation dispersion and circular dichroism studies, J. Biol. Chem. 266 (1991) 9835–9840.
[21] K.D. Hardman, R.C. Agarwal, M.J. Freiser, Manganese and calcium binding sites of concanavalin A, J. Mol. Biol. 5 (1982) 69–86.
[22] J.N. Sanders, S.A. Chenoweth, F.P. Schwarz, Effect of metal ion substitutions in concanavalin A on the binding of carbohydrates and on thermal stability, J. Inorg. Biochem. 70 (1998) 71–82.
[23] A. Chatterjee, D.K. Mandal, Quaternary association and reactivation of dimeric concanavalin A, Int. J. Biol. Macromol. 35 (2005) 103–109.
[24] S. Sinha, N. Mitra, G. Kumar, K. Bajaj, A. Surolia, Unfolding studies on soybean agglutinin and concanavalin A tetramers: a comparative account, Biophys. J. 88 (2005) 1300–1310.
[25] N. Mitra, V.R. Srinivas, T.N.C. Ramya, N. Ahmad, G.B. Reddy, A. Surolia, Conformational stability of legume lectins reflect their different modes of quaternary association: solvent denaturation studies on concanavalin A and winged bean acidic agglutin, Biochemistry 41 (2002) 9256–9263.
[26] J. Emsley, H.E. White, B.P. O'Hara, G. Oliva, N. Srinivasan, I.J. Tickle, T. L. Blundell, M.B. Pepys, S.P. Wood, Structure of pentameric human serum amyloid P component, Nature 367 (1994) 338–345.
[27] M.N. Pflumm, S. Beychok, Alkali and urea induced conformation changes in concanavalin A, Biochemistry 13 (1974) 4982–4987.
[28] Q. Xu, T.A. Keiderling, Trifluoroethanol-induced unfolding of concanavalin A: equilibrium and time-resolved optical spectroscopic studies, Biochemistry 44 (2005) 7976–7987.
[29] A.L. Fink, Protein aggregation: folding aggregates, inclusion bodies and amyloid, Fold. Des. 3 (1998) 9–23.
[30] J.S. Richardson, D.C. Richardson, Natural beta-sheet proteins use negative design to avoid edge-to-edge aggregation, Proc. Natl. Acad. Sci. U. S. A. 99 (2002) 2754–2759.
[31] T.K. Dam, R. Roy, S.K. Das, S. Oscarson, C.F. Brewer, Binding of multivalent carbohydrates to concanavalin A and Dioclea Grandiflora lectin, J. Biol. Chem. 275 (2000) 14230–14233.
[32] T.K. Dam, R. Roy, D. Page, C.F. Brewer, Negative cooperativity associated with binding of multivalent carbohydrates to lectins. Thermodynamic analysis of the "multivalency effect", Biochemistry 41 (2002) 1351–1358.
[33] T.K. Dam, R. Roy, D. Page, C.F. Brewer, Thermodynamic binding parameters of individual epitopes of multivalent carbohydrates to concanavalin A as determined by "reverse" isothermal titration microcalorimetry, Biochemistry 41 (2002) 1359–1363.
[34] S.L. Mangold, M.J. Cloninger, Binding of monomeric and dimeric concanavalin A to mannose-functionalized dendrimers, Org. Biomol. Chem. 4 (2006) 2458–2465.
[35] G. Tiegs, J. Hentschel, A. Wendel, A T cell-dependent experimental liver injury in mice inducible by concanavalin A, J. Clin. Invest. 90 (1992) 196–203.
[36] A. Ohta, M. Sitkovsky, Role of G-protein-coupled adenosine receptors in downregulation of inflammation and protection from tissue damage, Nature 414 (2001) 916–920.
[37] E. Song, S.K. Lee, J. Wang, N. Ince, N. Ouyang, J. Min, J. Chen, P. Shankar, J. Lieberman, RNA interference targeting Fas protects mice from fulminant hepatitis, Nat. Med. 9 (2003) 347–351.
[38] C. Moreno, T. Gustot, C. Nicaise, E. Quertinmont, N. Nagy, M. Parmentier, O. Le Moine, J. Deviere, H. Louis, CCR5 deficiency exacerbates T-cell-mediated hepatitis in mice, Hepatology 42 (2005) 854–862.
[39] T. Fukuda, A. Mogami, M. Hisadome, H. Komatsu, Therapeutic administration of Y-40138, a multiple cytokine modulator, inhibits concanavalin A-induced hepatitis in mice, Eur. J. Pharmacol. 523 (2005) 137–142.
[40] D.H. Cribbs, V.M. Kreng, J. Anderson, C.W. Cotman, Cross-linking of concanavalin receptors on cortical neurons induces programmed cell death, Neuroscience 75 (1996) 173–185.
[41] A.J. Anderson, C.J. Pike, C.W. Cotman, Differential induction of immediate early gene proteins in cultured neurons by beta-amyloid (Aβ): association of c-*jun* with Aβ-induced apoptosis, J. Neurochem. 65 (1995) 1487–1498.
[42] H. Naiki, K. Higuchi, M. Hosokawa, T. Takeda, Fluorometric determination of amyloid fibrils in vitro using the fluorescent dye, thioflavine T, Anal. Biochem. 177 (1989) 244–249.
[43] H. Naiki, F. Gejyo, Kinetic analysis of amyloid fibril formation, Methods Enzymol. 309 (1999) 305–318.
[44] M. Kudou, K. Shiraki, M. Takagi, Characterization of heat-induced aggregates of concanavalin A using fluorescent probes, Sci. Technol. Adv. Mater. 5 (2004) 339–341.
[45] J. Bouckaert, R. Loris, F. Poortmans, L. Wyns, Crystallographic structure of metal-free concanavalin A at 2.5Å resolution, Proteins 23 (1995) 510–524.
[46] J. Sanz-Aparicio, J. Hermoso, T.B. Grangeiro, J.J. Calvete, B.S. Cavada, The crystal structure of *Canavalia brasiliensis* lectin suggest a correlation between its quaternary conformation and its distinct biological properties from concanavalin A, FEBS Lett. 17 (1997) 114–118.
[47] A. Relini, C. Canale, S. Torrassa, R. Rolandi, A. Gliozzi, C. Rosano, M. Bolognesi, G. Plakoutsi, M. Bucciantini, F. Chiti, M. Stefani, Monitoring the process of HypF fibrillization and liposome permeabilization by protofibrils, J. Mol. Biol. 338 (2004) 943–957.
[48] A. Relini, R. Rolandi, M. Bolognesi, A. Gliozzi, M. Aboudan, G. Merlini, V. Bellotti, Ultrastructural organization of ex-vivo amyloid fibrils formed by the apolipoprotein A-I Leu174Ser variant: an atomic force microscopy study, Biochim. Biophys. Acta 1690 (2004) 33–41.
[49] M. Kudou, K. Shiraki, M. Takagi, Stretched-exponential analysis of heat-induced aggregation of apo–concanavalin A, Prot. J. 24 (2005) 193–199.
[50] J.W. Kelly, Amyloid fibril formation and protein misassembly: a structural quest for insights into amyloid and prion diseases, Structure 5 (1997) 595–600.
[51] H.A. Lashuel, Z. Lai, J.W. Kelly, Characterization of the transthyretin acid denaturation pathway by analytical ultracentrifugation: implications for wild type, V30M and L55P amyloid fibril formation, Biochemistry 37 (1998) 17851–17864.
[52] A. Quintas, M.J.M. Saraiva, R.M.M. Brito, The tetrameric protein transthyretin dissociates to a non-native monomer in solution, J. Biol. Chem. 274 (1999) 32943–32949.
[53] A. Quintas, D.C. Vaz, I. Cardoso, M.J.M. Saraiva, R.M.M. Brito, Tetramer dissociation and monomer partial unfolding precedes protofibril formation in amyloidogenic transthyretin variants, J. Biol. Chem. 276 (2001) 27207–27213.
[54] T.R. Foss, L. Wiseman, J.W. Kelly, The pathway by which the tetrameric protein transthyretin dissociates, Biochemistry 44 (2005) 15525–15533.
[55] F. Ferrone, Analysis of protein aggregation kinetics, Methods Enzymol. 309 (1999) 256–274.
[56] S.B. Padrick, A.D. Miranker, Islet amyloid: phase partitioning and secondary nucleation are central to the mechanism of fibrillogenesis, Biochemistry 41 (2002) 4694–4703.
[57] F. Librizzi, C. Rischel, The kinetic behavior of insulin fibrillation is determined by heterogeneous nucleation pathways, Protein Sci. 14 (2005) 3129–3134.
[58] M. Manno, E.F. Craparo, D. Bulone, V. Martorana, P.L. San Biagio, Kinetics of insulin aggregation: disentanglement of amyloid fibrillation from large-size cluster formation, Biophys. J. 90 (2006) 4585–4591.
[59] R. Carrotta, M. Manno, D. Bulone, V. Martorana, P.L. San Biagio, Protofibril formation of amyloid β-protein at low pH via a non-cooperative elongation mechanism, J. Biol. Chem. 280 (2005) 30001–30008.